# An almost periodic model of lead metabolism

# Un modelo casi periódico del metabolismo del plomo

Derik Castillo Guajardo[1], Osvaldo Osuna[2],

and José Geiser Villavicencio Pulido[1]

---

✉ Villavicencio Pulido: j.villavicencio@correo.ler.uam.mx

[1] División de Ciencias Biológicas y de la Salud, Depto. de Ciencias Ambientales.
Universidad Autónoma Metropolitana, Unidad Lerma.
Edo. de México, México.

[2] Instituto de Física y Matemáticas, Universidad Michoacana.
Michoacán, México.

## Abstract

A two compartmental almost periodic model is proposed to describe lead metabolism. Unlike other models proposed to analyze metal metabolism, all the rates involved in the model are assumed to be almost periodic functions, since it is very restrictive to assume that the input and output rates involved in lead metabolism are constant. From the analysis of the model, we prove that the model admits a unique almost periodic solution which is globally stable when some conditions over the parameters of the model are satisfied. Numerical simulations of the solutions of the model show that the use of constant or periodic rates in the modeling process, when almost periodic rates should actually be considered, can generate misleading predictions about the values of the variables. In such scenarios, misleading forecasts could be obtained that might lead decision-makers to design erroneous strategies, which can have negative impacts from a health perspective.

**Keywords:**

Lead metabolism, Metal metabolism, Almost periodic function, Cooperative systems, Global attractor

## Resumen

Se propone un modelo bicompartimental casi periódico para describir el metabolismo del plomo. A diferencia de otros modelos propuestos para analizar el metabolismo de metales, se supone que todas las tasas involucradas en el modelo son funciones casi periódicas, ya que es muy restrictivo asumir que las tasas de entrada y salida involucradas en el metabolismo del plomo son constantes. A partir del análisis del modelo, probamos que este admite una solución casi periódica única que es globalmente estable cuando se satisfacen ciertas condiciones sobre los parámetros del modelo. Las simulaciones numéricas de las soluciones del modelo muestran que el uso de tasas constantes o periódicas en el proceso de modelado, cuando en realidad deberían considerarse tasas casi periódicas, puede generar predicciones erróneas sobre los valores de las variables. En tales escenarios, se podrían obtener pronósticos engañosos que pueden llevar a los responsables de la toma de decisiones a diseñar estrategias equivocadas, lo cual puede tener impactos negativos desde una perspectiva de salud.

**Palabras Claves:**

Metabolismo del plomo, Metabolismo de metales, Función casi periódica, Sistemas cooperativos, Atractor global

## INTRODUCTION

**L**ead poisoning has been a critical public health concern in developing countries for at least 50 years. Lead has been recognized as one of the top ten chemicals of major public health concern. The main physiological consequences of lead exposure include disruption of heme synthesis, interference with Ca-mediated cellular processes, impaired mitochondrial respiration, and oxidative stress (Needleman, 2004; Flora *et al.*, 2012). The spectrum of clinical outcomes includes cognitive impairment, and developmental delays in children, as well as hypertension, renal dysfunction, and reproductive toxicity in adults (Gidlow, 2015).

Lead exposure can occur through various sources, including lead-based paint, contaminated soil, and dust (Assi *et al.*, 2016) as well as lead-based solder in water distribution systems (Jarvis and Fawell, 2021). It is estimated that 20% of total lead exposure in the United States occurs through drinking water. Importantly, current determination methods were found to underestimate lead concentration in water from faucets, both in households and schools (Triantafyllidou and Edwards, 2012). Lipsticks sold in Mexico but produced elsewhere, were found to contain $1.17 - 1.82$ ppm of lead (average 1.45 ppm). While these concentrations fell within the FDA regulations (10 ppm), lead in lipsticks from Ghana exceeded said limit, indicating potential neurotoxic effects (Saah *et al.*, 2024).

Bioaccumulation of lead across various tissues explains its systemic toxicity. The rate of bioaccumulation depends on the exposure route and duration, together with age, nutritional status, and genetic predisposition. Briefly, upon absorption by inhalation or ingestion, lead travels through the bloodstream, and is gradually deposited in mineralizing tissues such as bones and teeth. Other organs with detectable concentrations of lead include liver, kidneys, and brain. Lead leaves the body mainly through feces, with urine being a minor ways of excretion.

The dynamics of metal metabolism has been analyzed trough several types of mathematical models, including qualitative regulation models, stochastic models, multi-agent models, and differential equation models (Curis *et al.*, 2009). Importantly, the differential equation models are the most used. Typically, differential equations models of metal metabolism pay no special attention to the biochemical reactions between the metal and the human body. Instead, metal metabolism is viewed as smooth fluxes of matter and elimination processes that are modeled assuming a first order kinetic of diffusion processes. These assumptions lead to linear models whose solutions can be obtained analytically. Examples of application of linear differential models in the context of metal metabolism, include alkali metals such as lithium (Swann *et al.*, 1990), sodium (Levin and Patlak, 1972); alkaline earth metals like calcium (Aubert *et al.*, 1963), magnesium (Upton and Ludbrook, 2005), strontium (Bauer and Ray, 1958); transition metals including cadmium (Redeker *et al.*, 2004), chromium (O'Flaherty *et al.*, 2001),

cobalt (Kahle and Zauke, 2002), copper (Ferreira *et al.*, 2009), iron (McLaren *et al.*, 1995), mercury (Farris *et al.*, 2008), nickel (Luciani and Polig, 2007), ruthenium (Beresford *et al.*, 1998), silver (Beresford *et al.*, 1998), vanadium (Azay *et al.*, 2001), zinc (Yokoi *et al.*, 2003); lanthanides cerium (Beresford *et al.*, 1998), lanthanum (Bronner *et al.*, 2008); actinides such as americium Luciani and Polig (2007), plutonium Polig *et al.* (2000), uranium (Fisher *et al.*, 1991); post-transition metals like aluminum (Yokel and McNamara, 2001), lead (Pounds and Leggett, 1998) and the metalloid selenium (Patterson and Zech, 1992). All models mentioned assume constant transition rates.

Mathematical models describing the kinetics of lead metabolism rely on clinical data monitoring the concentration of lead in several compartments. Such models have proved critical for risk assessment, exposure estimation, and public health intervention. Foundational work such as the Rabinowitz three compartment model with constant coefficients, emphasized the dynamic equilibrium between compartments. Other models introduced more physiological realism (Leggett, 1993). For example, letting parameters depend on sex and age allows for simulation of lead kinetics across lifespan stages. More recently, models have incorporated tissue specific uptake and clearance rate, as well as mineral turnover rates, enhancing model applicability to environmental and exposure scenarios.

Modeling kinetics of lead metabolism in the human body trough differential equations with constant rates can be misleading, since the effects caused by both endogenous and exogenous factors involved in the lead metabolism are oversimplified. For example lead intake from various sources is not constant, due to intrinsic variations in each exposure route. As a consequence, the results obtained from linear models leave out scenarios that may be relevant from a health perspective. On top of that, traditional models with constant rates provide only a first glance at the dynamics of lead metabolism. This is particularly true in cases in which individuals are both periodically and aperiodically exposed to quantities of lead from non-constant sources so varied as diet or the atmosphere which can in turn alter the lead physiology in these individuals.

Therefore, the aim of this paper was to formulate and analyze a compartment model for lead metabolism kinetics with almost periodic rates. To incorporate biological mechanisms with oscillatory behaviors in the lead metabolism, we used an almost periodic model whose rates are given by linear combinations of trigonometric functions which are not necessarily synchronized. So, the use of almost periodic rates of transition between compartments offers a novel and important insight with explanatory potential. Almost periodic models have been used to understand enzymatic reactions (Díaz-Marín and Sánchez-Ponce, 2024), protein transcription dynamics (Díaz-Marín *et al.*, 2023) and neuronal mechanisms (Díaz-Marín *et al.*, 2025) among other biological phenomena when endogenous and exogenous stimuli give origin to oscillatory dynamics.

## THE ALMOST PERIODIC MODEL

In this section, we propose a compartmental almost periodic model to describe the dynamics of the lead metabolism in the human body. We constructed the model from Figure 1, a diagramatic model of lead metabolism proposed by Rabinowitz and coworkers (Rabinowitz *et al.*, 1976). Through this model, the authors analyzed the lead concentrations in blood, soft tissue and skeleton which are denoted by $X_1$, $X_2$ and $X_3$, respectively. Lead intake enters the bloodstream and then transits to soft tissues and bones. Lead exits the body through secretions.
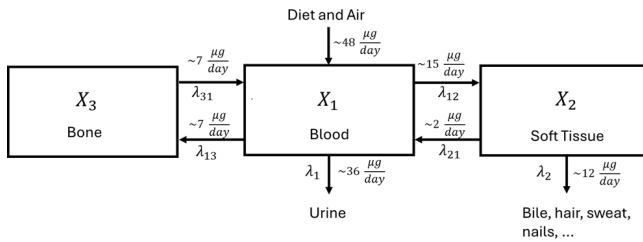


**Figure 1:** Diagramatic model of lead metabolism. The numerical values are the mean transition rates which were estimated from tracer an balance data from five healthy men Rabinowitz *et al.* (1976)

Rabinowitz et al. (Rabinowitz *et al.*, 1976) analyzed the compartment model described in Figure 1 and concluded that changes in lead concentration in bones are very slow in comparison with blood and soft tissue. Therefore, they constructed a mathematical model only with $X_1$ and $X_2$.

Similarly, we constructed a mathematical model of lead concentrations in blood and soft tissue by assuming that this system is input-output connected by mechanisms with an oscillatory behavior. To do this, we used transition rates given by almost periodic functions. The proposed model can be written as

$$\begin{aligned}
\frac{dX_1}{dt} &= \frac{A(t)}{M_1(t)} - \lambda_1(t)X_1 + \lambda_{21}(t)\frac{M_2(t)}{M_1(t)}X_2, \\
\frac{dX_2}{dt} &= \lambda_{12}(t)\frac{M_1(t)}{M_2(t)}X_1 - \lambda_2(t)X_2.
\end{aligned} \tag{1}$$

In model (1), $X_i$, for $i, j = 1, 2$ denotes lead concentration in compartment $i$ at time $t$, $M_i(t)$ is the mass of compartment $i$, $A(t)$ denotes the rate of recruitment of lead into compartment $X_1$ from outside the body, $\lambda_i(t)$ denotes the rate for the movement of lead out of compartment $i$. Finally, $\lambda_{ij}(t)$, with $j \neq i$, denotes the rate for movement from compartment $j$ to $i$.

## ALMOST PERIODIC FUNCTIONS IN COOPERATIVE SYSTEMS

In this first part we summarize some well known basic facts about the almost periodic functions and cooperative systems. Almost periodic functions are nowadays a very active research area. We give here only a very basic introduction to

the topic and refer the reader to (Bohr, 1947; Corduneanu, 1968) for further details.

**Definition 1** *A function* $\phi \in C^0(\mathbb{R})$ *is* almost periodic *if, for all* $\varepsilon > 0$ *there exist a set of real numbers* $T(\varepsilon) \subseteq \mathbb{R}$ *altogether with a length* $l(\varepsilon) > 0$ *such that for any interval of length* $l(\varepsilon)$, *there is at least one point* $\tau \in T(\varepsilon)$ *contained in that interval such that*

$$|\phi(x + \tau) - \phi(x)| < \varepsilon$$

*for each* $x \in \mathbb{R}$. *We will call numbers in* $T(\varepsilon)$ translation numbers *and a length for* $T(\varepsilon)$ *will be a number* $l(\varepsilon)$.

The above collection of every almost periodic functions will be denoted by $AP(\mathbb{R})$ which is a Banach space endowed with the usual $\sup-$norm. It is possible to associate to an almost periodic function $\varphi$ its unique Fourier series:

$$\varphi \sim \sum_{n \in \mathbb{N}} a(\lambda_n)e^{i\lambda_n x}.$$

The exponents $\lambda_n$ are called the frequencies of $\phi$. Another well-known result in this area is that, for every almost periodic function there exists the *mean value*

$$\mathscr{M}(\phi) := \lim_{T \to \infty} \frac{1}{T}\int_0^T \phi(x)dx,$$

this is a bounded linear function $\mathscr{M}: AP(\mathbb{R}) \to \mathbb{R}$ with the following properties:

1. $\phi \geq 0$ implies $\mathscr{M}[\phi] \geq 0$.

2. The Parseval equality holds:

$$\mathscr{M}[|\phi|^2] = \sum_{n \in \mathbb{N}} |a(\lambda_n)|^2.$$

Now we review some aspects about cooperative systems, for a brief introduction to cooperative systems see (Smith, 1995). For two points $u, v \in \mathbb{R}^2$ denote the partial order $u \leq v$ if $u_i \leq v_i$ for each $i$, also denote $u < v$ if $u \leq v$ and $u \neq v$. Let $f, g: \mathbb{R} \times D \subseteq \mathbb{R}^3 \to \mathbb{R}$ be a couple of differentiable and almost periodic functions on the first variable. We consider the system:

$$\begin{aligned}
x'(t) &= f(t, x(t), y(t)), \\
y'(t) &= g(t, x(t), y(t)),
\end{aligned} \tag{2}$$

where we suppose that $f(t, x, y), g(t, x, y)$ are both *uniformly almost periodic with respect to* $(x, y) \in C$ for every compact $C \subseteq D$, i.e., the set of translation numbers, $\tau(\varepsilon)$, is independent of $(x, y) \in C$.

More specifically, if $f$ have generalized Fourier expansions,

$$f(t, x, y) \sim \overline{f}(x, y) + \sum_{n=0}^{\infty} a(f, \lambda_n)\cos(\lambda_n t) + b(f, \lambda_n)\sin(\lambda_n t),$$

$f$ is uniformly almost periodic, whenever the coefficients $a(\cdot, \lambda_n), b(\cdot, \lambda_n)$ do not depend on $(x, y)$, see (Corduneanu, 1968), Chapter VI.

**Definition 2** *We say that* (2) *is of the* cooperative type, *if for every* $t \in \mathbb{R}$,

$$\frac{\partial f}{\partial y}(t, x, y) \geq 0, \ \frac{\partial g}{\partial x}(t, x, y) \geq 0.$$

*Moreover,* $(\xi(t), \eta(t))$ *is* sub-solution *if*

$$\xi'(t) \leq f(t, \xi(t), \eta(t)), \tag{3}$$
$$\eta'(t) \leq g(t, \xi(t), \eta(t)). \tag{4}$$

*Analogously, we define a* super-solution $(\Xi(t), H(t))$ *by reversing inequalities. A pair* $(\xi(t), \eta(t))$ *and* $(\Xi(t), H(t))$ *is* ordered *if*

$$\xi(t) \leq \Xi(t), \quad \eta(t) \leq H(t), \quad \forall t \in \mathbb{R}.$$

We will use the following result proved in (Díaz-Marín *et al.*, 2022).

**Theorem 1** *Suppose that* $(\xi(t), \eta(t))$ *and* $(\Xi(t), H(t))$ *is a sub-super-solution ordered pair of the cooperative ODE* (2). *Then, there exists an almost periodic solution satisfying* $\xi(t) < x(t) < \Xi(t)$ *and* $\eta(t) < y(t) < H(t)$. *The set of almost periodic solutions, having initial conditions in the rectangle* $\xi(0) < x(0) < \Xi(0)$ *and* $\eta(0) < y(0) < H(0)$, *is totally ordered, provided there is no equilibrium. If* $(\check{x}(t), \check{y}(t)), (\hat{x}(t), \hat{y}(t))$, *denote the minimal and maximal almost periodic solutions. Then*

$$\check{x}(t) \leq x(t) \leq \hat{x}(t), \quad \check{y}(t) \leq y(t) \leq \hat{y}(t).$$

Note that in the case where there is an equilibrium point, we could have an equilibrium instead of a genuine almost periodic orbit.

## RESULTS

As usual for an almost periodic function $v : \mathbb{R} \to \mathbb{R}$, we denote

$$v_* := \inf_{t \in \mathbb{R}} v(t) \ \text{ and } \ v^* := \sup_{t \in \mathbb{R}} v(t).$$

Now we state the main result for the almost periodic kinetic model given by (1).

**Theorem 2** *Assume* $A(t), M_i(t), \lambda_i(t)$ *and* $\lambda_{ij}(t)$ *are continuous almost-periodic functions (not all constant) with* $A_* > 0$, $M_{i*} > 0, \lambda_{i*} > 0, \lambda_{ij*} > 0$ *and that there is no equilibrium point of* (1) *with positive coordinates. Suppose further that*

$$\left(\frac{M_i \lambda_{ij}}{M_j}\right)^* < \lambda_{j*}, \ i \neq j, \text{ for } i, j = 1, 2. \tag{5}$$

*Then, there is a unique almost periodic solution* $(X_1, X_2)$ *of* (1) *whose components are positive. Also, any other solution of* (1) *with positive initial conditions converges to this almost periodic solution, when* $t \to \infty$.

Proof A careful examination shows us that system (1) is of cooperating type. Let us first establish the existence of at least one almost periodic solution, for this, we need to prescribe suitable sub- and super-solution pairs. To develop a sub-solution pair, we consider

$$(\xi(t), \eta(t)) = (\varepsilon, 0), \ \varepsilon > 0,$$

these functions satisfy the inequalities in (3), indeed

$$\xi'(t) = 0 \leq \left[\frac{A(t)}{M_1(t)} - \lambda_1 \varepsilon\right],$$
$$\eta'(t) = 0 \leq \left[\lambda_{12}\frac{M_1}{M_2} - \lambda_2(0)\right].$$

The right sides are positive for $\varepsilon > 0$ small enough. Thus we have a sub-solution pair.

For a super-solution pair; we consider

$$(\Xi(t), H(t)) = (N, N), \ N > 0,$$

these functions verify:

$$\Xi(t)'(t) = 0 \geq \frac{A(t)}{M_1} - \left[\lambda_{1*} + \left(\frac{M_2 \lambda_{21}}{M_1}\right)^*\right] N$$
$$\geq \frac{A(t)}{M_1} - \lambda_1 N + \left(\frac{M_2 \lambda_{21}}{M_1}\right) N.$$
$$H'(t) = 0 \geq N\left[\left(\frac{M_1 \lambda_{12}}{M_2}\right)^* - \lambda_{2*}\right]$$
$$\geq N\left[\frac{M_1 \lambda_{12}}{M_2} - \lambda_2\right].$$

By letting $N$ big enough and using (5), the right sides are negative, thus constituting a super-solution pair.

Therefore, by Theorem 1 there exists at least one almost periodic solution for system (1). This concludes the existence.

For uniqueness, we consider a maximal pair $(\hat{X}_1, \hat{X}_2)$ and minimal pair $(\check{X}_1, \check{X}_2)$ of almost periodic solutions. We just need to prove that $\hat{X}_1(t) = \check{X}_1(t)$ and $\hat{X}_2(t) = \check{X}_2(t)$. For which we will use the following well-known statement

**Claim 1** *Let* $\hat{\phi}, \check{\phi}$ *be almost periodic functions such that*

$$\hat{\phi}(t) \geq \check{\phi}(t) \geq 0, \qquad \mathcal{M}\left[\hat{\phi}\right] = \mathcal{M}\left[\check{\phi}\right].$$

*Then* $\hat{\phi}(t) = \check{\phi}(t)$ *for every* $t \in \mathbb{R}$.

Note that the mean $\mathcal{M}\left[(\hat{X}_i)'\right] = \mathcal{M}\left[(\check{X}_i)'\right] = 0$, then

$$\mathcal{M}\left[\frac{M_i \lambda_{ij}}{M_j}\left(\hat{X}_i - \check{X}_i\right)\right] = \mathcal{M}\left[\lambda_j\left(\hat{X}_j - \check{X}_j\right)\right], i \neq j. \tag{6}$$

Hence, from (6), we get

$$\lambda_{1*}\mathcal{M}\left[\hat{X}_1 - \check{X}_1\right] \leq \left(\frac{M_2 \lambda_{21}}{M_1}\right)^* \mathcal{M}\left[\hat{X}_2 - \check{X}_2\right]$$
$$\leq \frac{\left(\frac{M_2 \lambda_{21}}{M_1}\right)^*\left(\frac{M_1 \lambda_{12}}{M_2}\right)^*}{\lambda_{2*}}\mathcal{M}\left[\hat{X}_1 - \check{X}_1\right].$$

If $\mathscr{M}\left[\hat{X}_1 - \check{X}_1\right] > 0$, the above inequality contradicts the condition in (5). Therefore $\mathscr{M}\left[\hat{X}_1\right] = \mathscr{M}\left[\check{X}_1\right]$, whence $\hat{X}_1 = \check{X}_1$ by the Claim 1. This in turn implies that $\hat{X}_2 = \check{X}_2$ via (6).

For completeness, we will give proof of the above claim. <u>Proof</u> Since $\hat{\phi}(t), \check{\phi}(t)$ are almost periodic, then they are bounded. Hence,

$$0 \le \mathscr{M}\left[\hat{\phi}^2 - \check{\phi}^2\right] \le \mathscr{M}\left[(\hat{\phi} - \check{\phi})(\hat{\phi} + \check{\phi})\right]$$
$$\le (2\sup\{\hat{\phi}(t)\})\mathscr{M}\left[\hat{\phi} - \check{\phi}\right] = 0.$$

Therefore, $\mathscr{M}\left[\hat{\phi}^2\right] = \mathscr{M}\left[\check{\phi}^2\right]$. Thus,

$$\begin{aligned} 0 &\le& \mathscr{M}\left[(\hat{\phi} - \check{\phi})^2\right] \le 2\left(\mathscr{M}\left[\hat{\phi}^2\right] - \mathscr{M}\left[\hat{\phi}\check{\phi}\right]\right) \\ &\le& 2\left(\mathscr{M}\left[\hat{\phi}^2\right] - \mathscr{M}\left[\check{\phi}^2\right]\right) = 0. \end{aligned}$$

If we apply Parseval's Theorem on the sum of the squares of the Fourier coefficients of $\hat{\phi} - \check{\phi}$ we get $\hat{\phi} \equiv \check{\phi}$.   □

Finally, we can conclude the proof of Theorem 2.

From the first part, we can take an arbitrarily small subsolutions. Also we can take an arbitrarily large supersolutions. Thus we have a single almost periodic orbit which is an attractor at the entire set $\mathbb{R}^2_{>0}$. This completes the proof of Theorem 2.

   □

## NUMERICAL SIMULATIONS OF THE SOLUTIONS OF THE MODEL

In this section, examples of the behavior of the solutions of model (1) are shown. To do this, we use the following functions to model almost periodic scenarios.

$$\begin{aligned} A(t) &=& A_a\left(A_b + A_c\sin(A_d t) + A_e\cos(A_f t)\right), \\ M_1(t) &=& M_{1a}\left(M_{1b} + M_{1c}\sin(M_{1d}t) + M_{1e}\cos(M_{1f}t)\right), \\ M_2(t) &=& M_{2a}\left(M_{2b} + M_{2c}\sin(M_{2d}t) + M_{2e}\cos(M_{2f}t)\right), \\ \lambda_1(t) &=& \lambda_{1a}\left(\lambda_{1b} + \lambda_{1c}\sin(\lambda_{1d}t) + \lambda_{1e}\cos(\lambda_{3f}t)\right), \\ \lambda_2(t) &=& \lambda_{2a}\left(\lambda_{2b} + \lambda_{2c}\sin(\lambda_{2d}t) + \lambda_{2e}\cos(\lambda_{3f}t)\right), \\ \lambda_{12}(t) &=& \lambda_{3a}\left(\lambda_{3b} + \lambda_{3c}\sin(\lambda_{3d}t) + \lambda_{3e}\cos(\lambda_{3f}t)\right), \\ \lambda_{21}(t) &=& \lambda_{4a}\left(\lambda_{4b} + \lambda_{4c}\sin(\lambda_{4d}t) + \lambda_{4e}\cos(\lambda_{4f}t)\right). \end{aligned}$$
(7)

For the numerical simulations given in Figure 2, we use the following values of the parameters $A_a = 0.048, A_b = 1.0, A_c = 0.2, A_d = \sqrt{0.03}, A_e = 0.5, A_f = \sqrt{0.05}, M_{1a} = 0.754, M_{1b} = 1.0, M_{1c} = 0.1, M_{1d} = \sqrt{3}, M_{1e} = 0.7, M_{1f} = \sqrt{5}, M_{2a} = 2.985, M_{2b} = 1.0, M_{2c} = 0.005, M_{2d} = \sqrt{3}, M_{2e} = 0.004, M_{2f} = \sqrt{5}, \lambda_{1a} = 0.16, \lambda_{1b} = 1.0, \lambda_{1c} = 0.01, \lambda_{1d} = \sqrt{3}, \lambda_{1e} = 0.04, \lambda_{1f} = \sqrt{5}, \lambda_{2a} = 0.012, \lambda_{2b} = 1.0, \lambda_{2c} = 0.3, \lambda_{2d} = \sqrt{3}, \lambda_{2e} = 0.02, \lambda_{2f} = \sqrt{5}, \lambda_{3a} = 0.015, \lambda_{3b} = 1.0, \lambda_{3c} = 0.04, \lambda_{3d} = \sqrt{3}, \lambda_{3e} = 0.5, \lambda_{3f} = \sqrt{5}, \lambda_{4a} = 0.002, \lambda_{4b} = 1.0, \lambda_{4c} = 0.4, \lambda_{4d} = \sqrt{3}, \lambda_{4e} = 0.02, \lambda_{4f} = \sqrt{5}$.

With these values of the parameters, $\left(\frac{M_2\lambda_{21}}{M_1}\right)^* = 0.13534$ and $\left(\frac{M_1\lambda_{12}}{M_2}\right)^* = 0.0012756$ while $\lambda_1 = 0.1520414456$ and $0.008170694320$. Therefore, the conditions in Theorem 2 given by $\left(\frac{M_i\lambda_{ij}}{M_j}\right)^* < \lambda_{j*}, i \ne j$, are satisfied. So, the solutions of the model converge to a unique almost periodic attractor,

for all initial conditions. In Figure 2, we show this scenario using the initial conditions: $(0.0035, 0.98)$, $(10.0035, 0.85)$, and $(5.0035, 1.1)$.



(a)



(b)
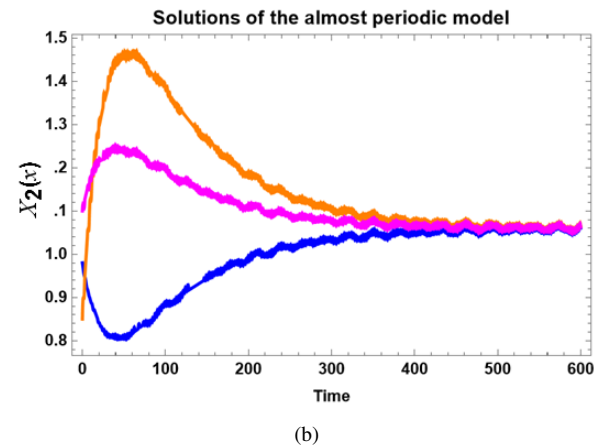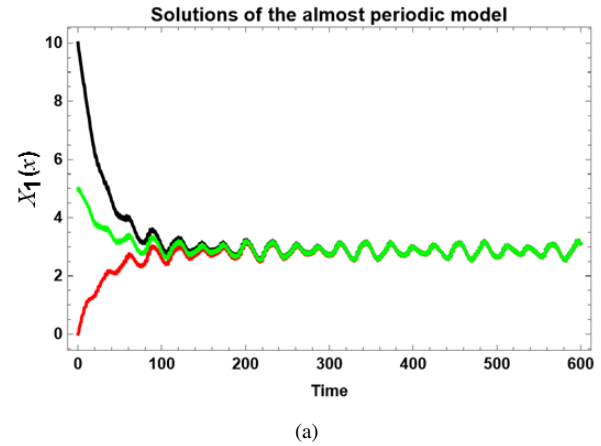
**Figure 2:** Solutions of the model converge to a global almost periodic attractor.

In Figure 3, we show the behavior of the solutions of the model when all its rates are assumed to be constant. To do this, the values of the parameters $A_j, M_{k,j}, \lambda_{s_j}$, in (7), are zero for $j = c, d$, $k = 1, 2$, and $s = 1, 2, 3, 4$. All other values of the parameters of the model are the same that those used in Figure 2. Notice that, the solutions of the model tend to a global attractor and the solutions of the model do not present an oscillatory behavior.
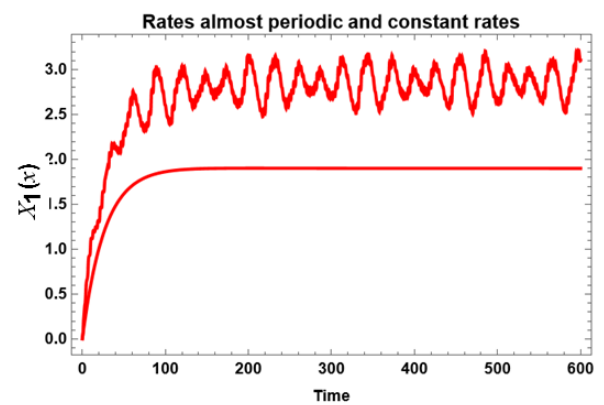
In Figure 4, solutions of the model are shown simultaneously for the cases of almost periodic rates and constant rates. The values of the parameters in these cases are the same used in the numerical simulations given in Figures 2 and 3, respectively. In this case, we use functions where the almost periodic rates oscillate around the values of the constant rates. In this case, the solutions of these scenarios are close at the beginning of time; however, the almost periodic solutions do not oscillate around the equilibrium solution of the model with constant rates at the long term.

Finally, for comparison purposes, in Figure 5, we show the solutions of the model in the almost periodic and periodic cases. For the almost periodic case, we use
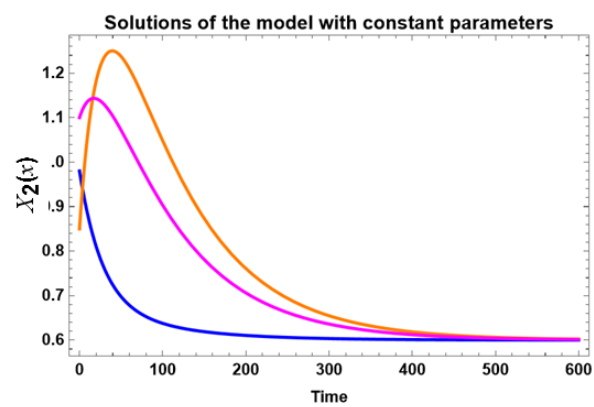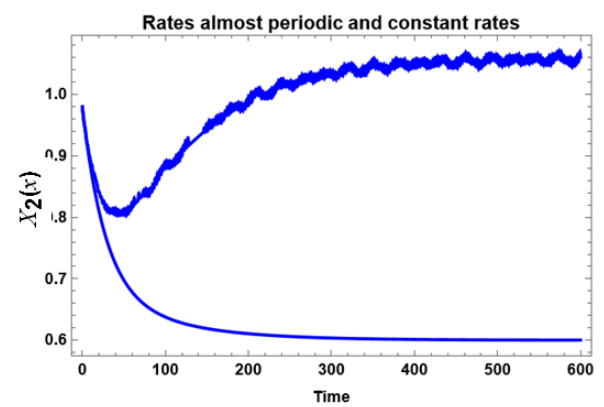
(a)
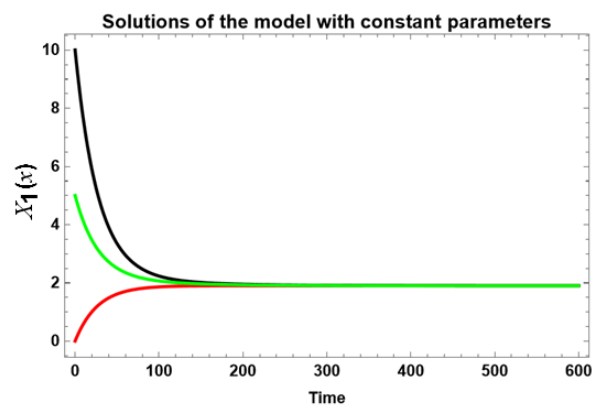


(b)

**Figure 3:** Solutions of the model tend to an equilibrium point when all its rates are constant.



(a)



(b)

**Figure 4:** Solutions of the model in the almost periodic and constant case.

one case given in Figure 2. In contrast, for the solutions in the periodic case, we used the following parameter values $A_4 = \sqrt{0.04}, A_6 = \sqrt{0.09}, M_{1c} = \sqrt{4}, M_{1d} = \sqrt{9}, M_{2c} = \sqrt{4}, M_{2d} = \sqrt{9}, \lambda_{1c} = \sqrt{4}, \lambda_{1d} = \sqrt{9}, \lambda_{2c} = \sqrt{4}, \lambda_{2d} = \sqrt{9}, \lambda_{3c} = \sqrt{4}, \lambda_{3d} = \sqrt{9}, \lambda_{4c} = \sqrt{4}, \lambda_{4d} = \sqrt{9}$. All other values of the parameters are the same as those used in Figure 2. Observe that the solutions in each case converge to a global attractor, which is an almost periodic or periodic solution, depending on whether the model is periodic or almost periodic. Notice that, the solutions of the model in both cases are very close initially; however, as time passes, there are intervals of time in which the solutions diverge.



(a)



(b)
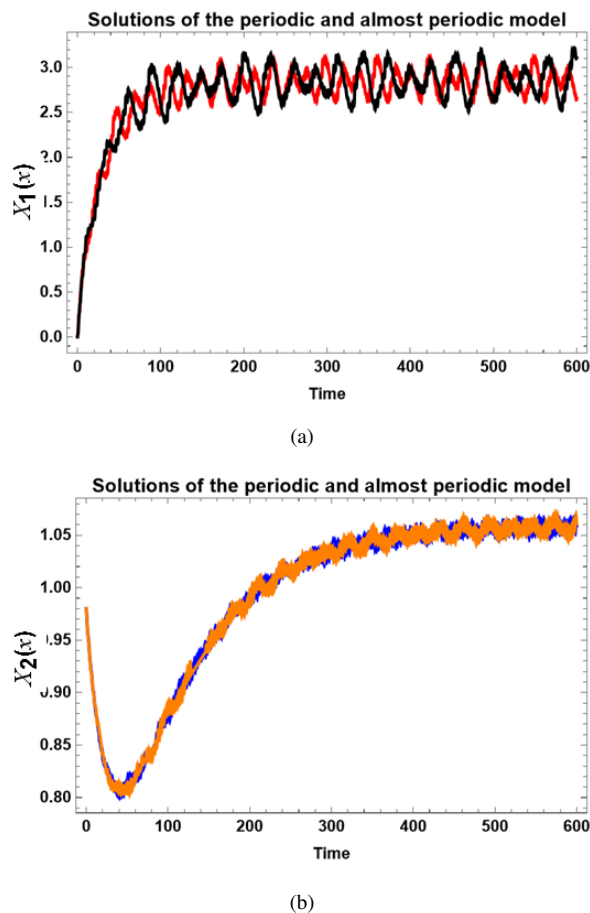
**Figure 5:** Solutions of the model in the almost periodic and periodic case.

We use the Sobol method, which is a variance-based global sensitivity analysis, to perform a sensitivity analysis of the solution $(X_1, X_2)$ of model (1), with respect to the parameters $\mathbf{x} = (A(t), M_1(t), M_2(t), \lambda_1(t), \lambda_2(t), \lambda_{12}(t), \lambda_{21}(t))$. This method decomposes the variance of the output of the model into fractions which can be attributed to sets of inputs using a sensitivity index. To obtain the results shown in Tables 1 and 2, we use the python library Salib (Herman and Usher, 2017) with the values of the parameters given by $A_a \in [0.28, 0.95], M_{1a} \in [1.1, 1.9], M_{2a} \in [2.7, 3.1], \lambda_{1a} \in [0.64, 0.68], \lambda_{2a} \in [0.72, 0.76], \lambda_{3a} \in [0.15, 0.35], \lambda_{4a} \in [0.18, 0.42]$. All other values of the parameters of the model

are given by those used in the simulation shown in Figure 2.

From an analysis of Tables 1 and 2, we can conclude that the variance in $X_1$ is dominated by the direct effect of the parameter $A(t)$ (accounting for almost 60%). Although there is an interaction component, the sum of the $S_1 (\approx 0.934)$ is very close to 1, indicating that the model is close to being additive. The parameters $\lambda_{12}(t)$ and $\lambda_{21}(t)$ are the ones that depend most on interactions to exert their total influence on $X_1$. The variance in $X_2(t)$ is explained almost entirely by $\lambda_{12}(t)$ and $A(t)$, but the role of interactions is more pronounced than in $X_1$. The parameter $\lambda_{12}(t)$ is not only the dominant one, but its interactions (0.0726) are the greatest source of non-additive variance in the model. This suggests that to control $X_2(t)$, it is necessary not only to estimate $\lambda_{12}(t)$ with precision, but also to understand how it combines with the variation of other parameters (especially $A(t)$).

## DISCUSSION

Lead is the second most toxic metal, naturally found in a very limited amount. Since lead serves industrial purposes, the magnitude of a society´s industrial sector can be thought as proportional to the scenarios of lead pollution. Examples of pollution are mining, and pollution of agricultural soils as well as water. Workers of, and neighborhoods around these industries often present health issues caused by long-term exposure (Raj and Das, 2023).

Mathematical models have been used to understand a large variety of problems derived from metal metabolism (Curis *et al.*, 2009). Among those, compartmental models, given by differential equations have been widely used to describe the evolution of a chemical species (a drug or lead concentration)

Table 1: Sobol Index Results for the solution $X_1(t)$ of the model.

| Parameter | $S_1$ ($\pm$ IC) | $S_T$ ($\pm$ IC) | Interaction ($S_T - S_1$) |
|---|---|---|---|
| $A(t)$ | $0.5969 \pm 0.0324$ | $0.6322 \pm 0.0278$ | $0.0353$ |
| $M_1(t)$ | $0.1524 \pm 0.0176$ | $0.1724 \pm 0.0086$ | $0.0199$ |
| $M_2(t)$ | $0 \pm 0$ | $0 \pm 0$ | $0$ |
| $\lambda_1(t)$ | $0.0052 \pm 0.0039$ | $0.0070 \pm 0.0004$ | $0.0018$ |
| $\lambda_2(t)$ | $0.0008 \pm 0.0014$ | $0.0012 \pm 0.0001$ | $0.0004$ |
| $\lambda_{12}(t)$ | $0.0935 \pm 0.0154$ | $0.1243 \pm 0.0078$ | $0.0308$ |
| $\lambda_{21}(t)$ | $0.0912 \pm 0.0140$ | $0.1248 \pm 0.0079$ | $0.0335$ |

Table 2: Sobol Index Results for the solution $X_2(t)$ of the model.

| Parameter | $S_1$ ($\pm$ IC) | $S_T$ ($\pm$ IC) | Interaction ($S_T - S_1$) |
|---|---|---|---|
| $A(t)$ | $0.3823 \pm 0.0258$ | $0.4361 \pm 0.0252$ | $0.0538$ |
| $M_1(t)$ | $0 \pm 0$ | $0 \pm 0$ | $0$ |
| $M_2(t)$ | $0.0060 \pm 0.0041$ | $0.0077 \pm 0.0006$ | $0.0017$ |
| $\lambda_1(t)$ | $0.0049 \pm 0.0032$ | $0.0067 \pm 0.0005$ | $0.0018$ |
| $\lambda_2(t)$ | $0.0051 \pm 0.0031$ | $0.0070 \pm 0.0005$ | $0.0019$ |
| $\lambda_{12}(t)$ | $0.4583 \pm 0.0297$ | $0.5309 \pm 0.0284$ | $0.0726$ |
| $\lambda_{21}(t)$ | $0.0609 \pm 0.0134$ | $0.0945 \pm 0.0071$ | $0.0336$ |

(a)



(b)
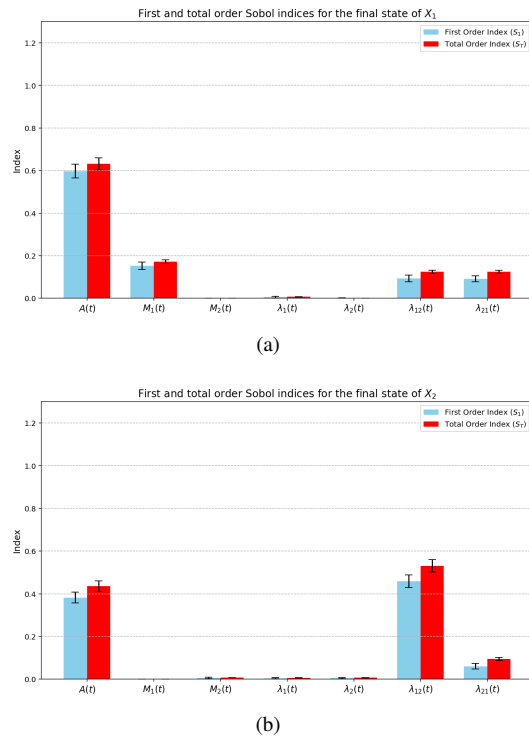
**Figure 6:** Cases (a) and (b) show the Sobol indices for the solutions $X_1$ and $X_2$ of model (1), respectively. The calculated indices, determined for several $t_i$ values, were found to be independent of $t_i$.

in any compartment of the body. To do this, modelers usually assume that diffusion between compartments follows-first order kinetics, in which transition rates are assumed constant. The resulting model is linear independently of its complexity. As a consequence, its analytical solution can be obtained and the concentration of the chemical species is known at all times. The usefulness of linear models depend on its assumptions being met. When first order kinetics do not apply, a linear model does not adequately describes the dynamics of the chemical species among compartments. This is the case of environmental drives, which affect some transition rates in the modelling process.

In this work, we propose an almost periodic differential equation model that generalizes the model for lead metabolism proposed in (Rabinowitz *et al.*, 1976). For this purpose, the rates of the model were taken as almost periodic functions. The physiological basis rely primarily on circadian clocks, as well as nutritional status: Intestinal absorption of lead is known to increase in the fasted state, and with iron/calcium deficiency (Ragan, 1983). Therefore, lead intake is expected to oscillate for populations with seasonal food insecurity, or regular dietary cycles. Additionally, lead concentration in blood is likely to follow a circadian rhythm: Markers of bone resorption peak at night/early morning (Bjarnason *et al.*, 2002). This means that bone-stored lead released into plasma peaks on an almost daily basis. Renal excretion is also known to show circadian

rhythmicity: urinary flow as well as solute excretion (including metals) decrease during the night (Solocinski and Gumz, 2015), adding to the concentration of lead in peripheral blood. Other sources of variability have also been detected. For example, maternal blood lead is known to increase during pregnancy. In this context, bone contributes a large fraction of the blood lead levels (Gulson *et al.*, 1997). In summary, lead metabolism is not constant, as early models portrayed. Rates of metabolic intake, deposition and excretion are likely to be under the influence of at least two almost periodic drivers, supporting our approach to the mathematical modelling of lead dynamics in the human body.

From an analysis of the existence and uniqueness of almost periodic solutions of the model, we proved that the model admits a unique almost periodic solution when the conditions in Theorem 2 are satisfied. We further proved that this almost periodic solution is a global attractor. Therefore, for every initial condition, the solutions converge to this almost periodic attractor; see Figure 2. Importantly, we showed that the choice of constant over almost periodic rates has a profound effect on the overall dynamics. In particular, constant rates tend to underestimate lead concentration when compared to almost periodic rates (Figure 4). Notice that solutions associated with both scenarios are close at the beginning of time, but they separate as time goes by. Through numerical results, in Figure 4, we show that small variations in the rates of the model lead to very different scenarios, which means that health decision makers must be cautious when interpreting model outputs obtained from clinical data, due to natural variation.

A similar situation was observed when comparing periodic and almost periodic rates. A side by side comparison (Figure 5) shows that the concentration of lead can be either under or overestimated by the model with periodic rates. In Figure 5, it is shown that the solutions of the model are close at the beginning of time; however, in future times, there are intervals of time in which the solutions are close and there are intervals in which they separate. Through these scenarios, we show that misleading forecasts can occur if periodic or constant rates are used to model lead metabolism since the input and output of lead in the body are neither constant nor periodic. In such a situation modeling lead metabolism with almost periodic model might be a better alternative.

From the Sobol analysis, we can conclude that $X_1$ is more sensitive to the parameter $A(t)$, while $X_2$ is more sensitive to changes in $\lambda_{12}(t)$ together with its other interactions, especially with the parameter $A(t)$. That is, for $X_1$, the sensitivity is primarily linear with respect to $A(t)$, whereas for $X_2$, the sensitivity is nonlinear.

Lead metabolism has been analyzed in different compartments such as bone, blood and soft tissues or through other refinements; for example, for one in which soft tissue is subdivided into liver, kidneys and neural tissue or one in which mineralized tissue can be subdivided into bones and teeth. Therefore, future refinements of our present study may include additional compartments.

# References

Assi, M.A., Hezmee, M.N., Haron, A.W., Sabri, M.Y. and Rajion, M.A. (2016) 'The detrimental effects of lead on human and animal health'. *Veterinary world*, 9(6), pp. 660–671. doi:doi:10.14202/vetworld.2016.660-671.

Aubert, J.P., Bronner, F. and Richelle, L.J. (1963) 'Quantitation of calcium metabolism'. *Theory Journal of Clinical Investigation*, 42(6), pp. 885–897.

Azay, J., Bre' s, J., Krosniak, M., Teissedre, P., Cabanis, J., Serrano, J.J. and Cros, G. (2001) 'Vanadium pharmacokinetics and oral bioavailability upon single-dose administration of vanadyl sulfate to rats'. *Fundamental and Clinical Pharmacology*, 15(5), pp. 313–324.

Bauer, G.C.H. and Ray, R.D. (1958) 'Kinetics of strontium metabolism in man'. *The Journal of Bone and Joint Surgery*, 40A(1), pp. 171–186.

Beresford, N.A., Crout, N.M.J., Mayes, R.W., Howard, B.J. and Lamb, C.S. (1998) 'Dynamic distribution of radioisotopes of cerium, ruthenium and silver in sheep tissues'. *Journal of Environmental Radioactivity*, 38(3), pp. 317–338.

Bjarnason, N.H., Henriksen, E.E.G., Alexandersen, P., Christgau, S., Henriksen, D.B. and Christiansen, C. (2002) 'Mechanism of circadian variation in bone resorption'. *Bone*, 30(1), pp. 307–313.

Bohr, H. (1947) *Almost Periodic Functions*. New York, N.Y.: Chelsea Pub Co.

Bronner, F., Slepchenko, B.M., Pennick, M. and Damment, S.J.P. (2008) 'A model of the kinetics of lanthanum in human bone, using data collected during the clinical development of the phosphate binder lanthanum carbonate'. *Clinical Pharmacokinetics*, 47(8), pp. 543–552.

Corduneanu, C. (1968) *Almost Periodic Functions*. New York: Interscience Publishers.

Curis, E., Nicolis, I., Bensaci, J., Deschamps, P. and Bénazeth, S. (2009) 'Mathematical modeling in metal metabolism: Overview and perspectives'. *Biochimie*, 91, pp. 1238–1254. doi:doi:10.1016/j.biochi.2009.06.019.

Díaz-Marín, H.G., López-Hernández, F. and Osuna, O. (2022) 'Almost periodic solutions for seasonal cooperative systems'. *Annales Polonici Mathematic*, 128(1), pp. 1–14. doi:doi:10.4064/ap210128-19-8.

Díaz-Marín, H.G., Osuna, O. and Villavicencio-Pulido, J.G. (2025) 'A bidirectional associative memory model with almost periodic endogenous and exogenous stimuli'. *Journal of Mathematical Modeling*, 13(1), pp. 33–48.

Díaz-Marín, H., Osuna, O. and Villavicencio-Pulido, G. (2023) 'An oscillatory model for globally stable protein transcription dynamics'. *J. Biol. Syst.*, 31, pp. 1–15.

Díaz-Marín, H. and Sánchez-Ponce, J.L. (2024) 'Intraspecific andmonotone enzyme catalysis with oscillatory substrate and inhibitor supplies'. *Journal of Mathematical Chemistry*, 62, pp. 2160–2190. doi:doi:10.1007/s10910-024-01630-8.

Farris, F., Kaushal, A. and Strom, J.G. (2008) 'Inorganic mercury pharmacokinetics in man: a two-compartment model'. *Toxicological and Environmental Chemistry*, 90(3), pp. 519–533.

Ferreira, D., Ciffroy, P., Tusseau-Vuillemin, M.H., Garnier, C. and Garnier, J.M. (2009) 'Modelling exchange kinetics of copper at the water-aquatic moss (Fontinalis antipyretica) interface: influence of water cationic composition (Ca, Mg, Na and pH)'. *Chemosphere*, 74(8), pp. 1117–1124.

Fisher, D.R., Kathren, R.L. and Swint, M.J. (1991) 'Modified biokinetic model for uranium from analysis of acute exposure to UF6'. *Health Physics*, 60(3), pp. 335–342.

Flora, G., Gupta, D. and Tiwari, A. (2012) 'Toxicity of lead: A review with recent updates'. *Interdisc Toxicol.*, 5(2), pp. 47–58. doi:doi:10.2478/v10102-012-0009-2.

Gidlow, D.A. (2015) 'Lead toxicity'. *Occup Med (Lond).*, 65(5), pp. 348–356. doi:doi:10.1093/occmed/kqv018.

Gulson, B., Jameson, C., Mahaffey, K., Mizon, K., Korsch, M. and Vimpani, G. (1997) 'Pregnancy increases mobilization of lead from maternal skeleton'. *Journal of Laboratory and Clinical Medicine*, 130(1), pp. 51–62.

Herman, J. and Usher, W. (2017) 'SALib: An open-source python library for sensitivity analysis'. *J. Open Res. Softw.*, 2(9), p. 97.

Jarvis, P. and Fawell, J. (2021) 'Lead in drinking water – An ongoing public health concern?' *Current Opinion in Environmental Science & Health*, 20, 100239. doi:doi:10.1016/j.coesh.2021.100239.

Kahle, J. and Zauke, G.P. (2002) 'Bioaccumulation of trace metals in the copepod Calanoides acutus from the Weddel Sea (Antarctica): comparison of two compartment and hyperbolic toxicokinetic models'. *Aquatic Toxicology*, 59, pp. 115–135.

Leggett, R.W. (1993) 'An age-specific kinetic model of lead metabolism in humans'. *Environmental Health Perspectives*, 101(7), pp. 598–616. doi:doi:10.1289/ehp.93101598.

Levin, V. and Patlak, C.S. (1972) 'A compartmental analysis of 24Na kinetics in rat cerebrum, sciatic nerve and cerebrospinal fluid'. *Journal of Physiol*, 224, pp. 559–581.

Luciani, A. and Polig, E. (2007) 'Surface-seeking radionuclides in the skeleton: current approach and recent developments in biokinetic modelling for humans and beagles'. *Radiation Protection and Dosimetry*, 127(1-4), pp. 140–143.

McLaren, G.D., Nathanson, M.H. and Saidel, S.M. (1995) *Kinetic Models of Trace Element and Mineral Metabolism During Development*, chap. Compartmental analysis of intestinal iron absorption and mucosal iron kinetics. CRC press, pp. 187–204.

Needleman, H. (2004) 'Lead poisoning'. *Annu Rev Med.*, 55, pp. 209–222. doi:doi:10.1146/annurev.med.55.091902.103653.

O'Flaherty, E.J., Kerger, B.D., Hays, S.M. and Paustenbach, D.J. (2001) 'A physiologically based model for the ingestion of chromium(III) and chromium(VI) by humans'. *Toxicological Sciences*, 60(2), pp. 196–213.

Patterson, B. and Zech, L.A. (1992) 'Development of a model for selenite metabolism in humans'. *Journal of Nutrition*, 122, pp. 709–714.

Polig, E., Bruenger, F., Lloyd, R. and Miller, S.C. (2000) 'Biokinetic and dosimetric model of plutonium in the dog'. *Health Physics*, 78(2), pp. 182–190.

Pounds, J.G. and Leggett, R.W. (1998) 'The ICRP age-specific biokinetic model for lead: validations, empirical comparisons, and explorations'. *Environmental Health Perspectives*, 106, pp. 1505–1511.

Rabinowitz, M.B., Wetherill, G.W. and Kopple, J.D. (1976) 'Kinetic Analysis of Lead Metabolism in Healthy Humans'. *The Journal of Clinical Investigation*, 58, pp. 260–270.

Ragan, H.A. (1983) 'The bioavailability of iron, lead and cadmium via gastrointestinal absorption: A review'. *Science of The Total Environment*, 28(1-3), pp. 317–326.

Raj, K. and Das, A.P. (2023) 'Lead pollution: Impact on environment and human health and approach for a sustainable solution'. *Environmental Chemistry and Ecotoxicology*, 5, pp. 79–85. doi:doi:10.1016/j.enceco.2023.02.001.

Redeker, E.S., Bervoets, L. and Blust, R. (2004) 'Dynamic model for the accumulation of cadmium and zinc fromwater and sediment by the aquatic oligochaete, Tubifex tubifex'. *Environmental Science and Technology*, 38(23), pp. 6193–6200.

Saah, S.A., Boadi, N.O., Saki, P. and Smith, Q.Q. (2024) 'Human health risks of lead, cadmium, and other heavy metals in lipsticks'. *Heliyon*, 10(23), e40576. doi:doi:10.1016/j.heliyon.2024.e40576.

Smith, H.L. (1995) *Monotone Dynamical Systems: an introduction to the theory of competitive and cooperative systems*. AMS.

Solocinski, K. and Gumz, M.L. (2015) 'The Circadian Clock in the Regulation of Renal Rhythms'. *J Biol Rhythms*, 6(30), pp. 470–486.

Swann, A.C., Berman, N., Frazer, A., Koslow, S.H., Maas, J.W., Pandey, G.N. and Secunda, S. (1990) 'Lithium distribution in mania: single-dose pharmacokinetics and sympathoadrenal function'. *Psychiatry Research*, 32(1), pp. 71–84.

Triantafyllidou, S. and Edwards, M. (2012) 'Lead (Pb) in Tap Water and in Blood: Implications for Lead Exposure in the United States'. *Critical Reviews in Environmental Science and Technology*, 42(13), pp. 1297–1352. doi:doi:10.1080/10643389.2011.556556.

Upton, R.N. and Ludbrook, G.L. (2005) 'Pharmacokinetic–pharmacodynamic modelling of the cardiovascular effects of drugs – method development and application to magnesium in sheep'. *BMC Pharmacology*, 5.

Yokel, R.A. and McNamara, P.J. (2001) 'Aluminium toxicokinetics: an updated minireview'. *Pharmacology and Toxicology*, 88(4), pp. 159–

167.

Yokoi, K., Egger, N.G., Ramanujam, V.M.S., Alcock, N.W., Dayal, H.H., Penland, J.G. and Sandstead, H.H. (2003) 'Association between plasma zinc concentration and zinc kinetic parameters in premenopausal women'. *American Journal of Physiology: Endocrinol Metab.*, 285, E1010–E1020.